Rewetting of an infinite tube with a uniform heating

A. K. Satapathy, R. K. Sahoo

Department of Mechanical Engineering
National Institute of Technology
Rourkela -769008
rksahoo@nitrkl.ac.in

Abstract The two-dimensional quasi-steady conduction equation governing conduction controlled rewetting of an infinite tube, with outer surface flooded and the inside surface subjected to a constant heat flux, has been solved by Wiener–Hopf technique. The solution yields the quench front temperature as a function of various model parameters such as Peclet number, Biot number and dimensionless heat flux. Also, the dryout heat flux is obtained by setting the Peclet number equal to zero, which gives the maximum sustainable heat flux to prevent the dryout of the coolant.

List of symbols

B	Biot number
C	specific heat
h	heat transfer coefficient
k	thermal conductivity
L	length of the tube
Pe	Peclet number
q	heat flux
Q	dimensionless heat flux
s	half of the Peclet number
t	time
T	temperature
u	quench front velocity
R, Z	physical coordinates
$\bar{r}, \bar{z}$	coordinates in quasi-steady state
r, z	dimensionless coordinates in quasi-steady state

Greek

δ	radius ratio
θ	dimensionless temperature
ρ	density

Subscripts

0	quench front
1	wet region
2	dry region
s	saturation
w	wall condition

1 Introduction

The process of quenching of hot surfaces is of practical importance in nuclear and metallurgical industries. For instance, in the event of a postulated loss-of-coolant accident (LOCA) in water cooled reactors, the clad surface of the fuel elements may reach very high temperature because the residual core heat cannot be removed adequately by the surrounding steam. In order to bring the reactor to a cooled shutdown condition, an emergency core cooling system is activated to reflood the core. However, the injected coolant does not immediately wet the cladding surface because a stable vapor blanket will prevent the liquid–solid contact. The maximum surface temperature when the coolant establishes contact with the hot surface is the rewetting or quench front temperature. When the clad surface is below the quench front temperature, rewetting occurs. Also, quenching phenomenon is of considerable practical interest in many other engineering applications, such as start-up of LNG pipe lines, filling of cryogenic vessels at room temperature, drying out of evaporator tubes and heat treatment of various materials.

During the cooling process, a local wet patch is instantaneously formed which eventually develops into a steadily moving quench front. As the quench front moves along the hot solid, two regions can be identified: a dry region ahead of the quench front and a wet region behind the quench front. In conduction-controlled rewetting analysis, it is believed that conduction of heat in the solid from dry region to wet region is the dominant mechanism of heat removal, which results in a lowering of the surface temperature immediately downstream of the quench front and causes the quench front to progress further. The upstream end of the solid is cooled by convection to the contacting liquid, while its downstream end is cooled by heat transfer to a mixture of vapor and entrained liquid droplets, called precursory cooling.

The two-dimensional rewetting model for two-region heat transfer with a step change in heat transfer coefficient at the quench front has been solved for a single slab (Levine 1982; Olek 1988; Tien and Yao 1975) and for a composite slab (Olek 1994). Rewetting models in the cylindrical geometry have been solved for a solid rod (Evans 1984), for a tube with an insulated core (Chakrabarti 1986) and for a composite tube (Olek 1989). In the single slab/tube model the unwetted region is considered to be adiabatic, whereas in case of a composite slab/tube a three-layer composite is considered to simulate the fuel and the cladding separated by a gas-filled gap between them. The

solution methods commonly employed are Wiener–Hopf technique. The two-dimensional rewetting model for a single slab with a uniform heat flux and precursory cooling has been solved by an approximate integral method (Yao 1977). The one-dimensional rewetting model with a uniform heat flux has been solved for a smooth plate (Peng and Peterson 1992) and for both smooth and grooved plates (Chan and Zhang 1994), considering the dry region to be adiabatic.

The analysis of rewetting of a hot surface with a specified boundary heat flux and the dryout induced by this heat flux is of specific interest while considering the decay heating of a nuclear fuel (Yao 1977) or in the design of heat pipes for thermal radiators (Peng and Peterson 1992; Chan and Zhang 1994). Chan and Zhang (1994) observed that the existence of heat flux on the wall poses an unsteady state solution for the heat conduction equation, even after the equation is transformed to the Lagrangian coordinate moving with the quench front. In this respect, they also considered the rewetting velocity as well as the plate temperature (at far ahead of the quench front) to be time variant. In the present paper, however, precursory cooling in the dry region has been included in the boundary condition in order to consider the quasi-steady state conduction equation, as described in the text. Further, reported literature on analytical investigations indicates that Wiener–Hopf solution for the rewetting model with a boundary heat flux does not exist. In the present analysis, Wiener–Hopf technique has been employed because of its accuracy and computational simplicity. Besides, the singularity arising due to the discontinuous boundary conditions (as in the case of a quenching problem) can be readily resolved by the Wiener–Hopf technique.

In the present study, the physical model consists of an infinitely extended vertical tube with outer surface flooded and the inner surface subjected to a uniform heat flux. The model assumes constant but different heat transfer coefficients for the wet and dry regions on the flooded side. The two-dimensional quasi-steady conduction equation governing the conduction-controlled rewetting of the infinite-tube has been solved by the Wiener–Hopf technique. The present solution involves the exact decomposition of the kernel function, in order that the solution may be valid for the entire range of the parameters used in the model. The solution is shown to be easily reduced to the cases of solid cylinder and tube with an insulated inner core and, thus, its correctness is checked. Numerical results for the quench front temperature are depicted in the graphical form for a wide range of model parameters.

2 Mathematical model

The two-dimensional transient heat conduction equation for the tube is

$$\frac{1}{R}\frac{\partial}{\partial R}\left(R\frac{\partial T}{\partial R}\right)+\frac{\partial^2 T}{\partial Z^2}=\frac{\rho C}{k}\frac{\partial T}{\partial t}$$
$$R_1 < R < R_2 \quad 0 < Z < L \quad L \to \infty \qquad (1)$$

where L is the length of the tube and R_1, R_2 are inner and outer radius of the tube. The density, specific heat and thermal conductivity of the tube material are ρ, C and k respectively. The origin of the coordinate frame is at the bottom point on the axis of the tube. To convert this transient equation into a quasi-steady state equation, the following transformation is used.

$$\bar{r} = R \quad \bar{z} = Z - ut$$

where u is the constant quench front velocity and $\bar{r}$ and $\bar{z}$ are radial and axial coordinates respectively (Fig. 1a). Thus the transformed heat conduction equation for a frame of reference $(\bar{r}, \bar{z})$ moving with the quench front at this velocity is

$$\frac{1}{\bar{r}}\frac{\partial}{\partial \bar{r}}\left(\bar{r}\frac{\partial T}{\partial \bar{r}}\right)+\frac{\partial^2 T}{\partial \bar{z}^2}+\frac{\rho C u}{k}\frac{\partial T}{\partial \bar{z}}=0$$
$$R_1 < \bar{r} < R_2 \quad -\infty < \bar{z} < \infty \qquad (2)$$

In conduction-controlled rewetting analysis the effect of coolant mass flux, coolant inlet subcooling and its pressure gradient etc. are not considered explicitly, but only implicitly in terms of wet region heat transfer coefficient,

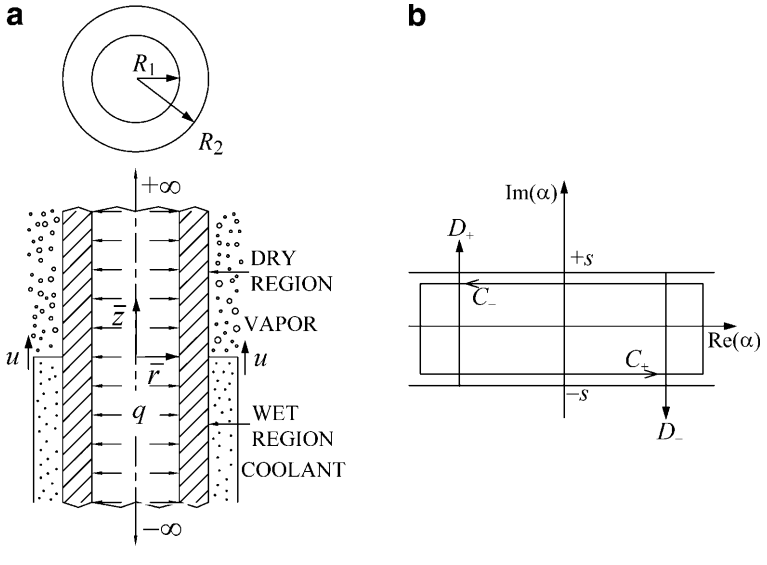

Fig. 1. (**a**) Physical domain of infinite tube, (**b**) common strip of analyticity in the complex Fourier plane

which is incorporated in the boundary condition. In the present study, the heat transfer coefficient h_1 is assumed to be constant over the entire wet region. The coolant temperature is taken to be equal to its saturation temperature T_s. On the dry side of the tube, the wall is cooled by the surrounding vapor. This cooling effect is very small as compared to that of wet region and is usually neglected in many rewetting models. However, this small cooling mechanism is very significant and essential in the rewetting analysis with boundary heat flux and cannot be neglected. The heat transfer coefficient accounting for both convective and radiative cooling effects on the dry side is assumed equal to h_2, a constant, which is smaller than h_1. The temperature of the surrounding vapor is assumed equal to T_w, which can be interpreted as the initial temperature of the tube without a heating. The rewetting (quench front) temperature is denoted by T_0.

The far-field boundary conditions may be derived with the assumption that the temperature field is sufficiently flat in the axial direction at infinity (Yao 1977). Therefore, the first and second derivatives of temperature in $\bar{z}$-direction (i.e. $\partial T/\partial \bar{z}$ and $\partial^2 T/\partial \bar{z}^2$) may be neglected at infinity ($\bar{z} \to \pm\infty$). The above two assumptions are adequate to prescribe the temperature at infinity. The corresponding boundary conditions then become

$$\begin{aligned} T &= T_s + \frac{q}{h_1}\frac{R_1}{R_2} + \frac{qR_1}{k}\ln\left(\frac{R_2}{\bar{r}}\right) \quad \text{at } \bar{z} \to -\infty \\ T &= T_w + \frac{q}{h_2}\frac{R_1}{R_2} + \frac{qR_1}{k}\ln\left(\frac{R_2}{\bar{r}}\right) \quad \text{at } \bar{z} \to +\infty \end{aligned} \tag{3}$$

It may be verified that for no heat flux condition with adiabatic dryside (by setting $q = 0$, $h_2 = 0$ and $q/h_2 = 0$), the boundary conditions in Eq. (3) reduces to that of conventional two-region model (Chakrabarti 1986; Olek 1989). The boundary conditions in Eq. (3) suggest that precursory cooling in the dry region cannot be neglected in case the tube wall is subjected to a heat flux. Equation (2) can be expressed in the following dimensionless form.

$$\frac{1}{r}\frac{\partial}{\partial r}\left(r\frac{\partial\theta}{\partial r}\right) + \frac{\partial^2\theta}{\partial z^2} + \mathrm{Pe}\frac{\partial\theta}{\partial z} = 0 \qquad \delta < r < 1 \quad -\infty < z < \infty \tag{4}$$

where δ is the radius ratio. The associated boundary conditions are

$$\begin{aligned} &\frac{\partial\theta}{\partial r} + Q = 0 \quad \text{at } r = \delta \quad -\infty < z < \infty \\ &\frac{\partial\theta}{\partial r} + \mathrm{B}_1\theta = 0 \quad \text{at } r = 1 \quad z < 0 \\ &\frac{\partial\theta}{\partial r} + \mathrm{B}_2(\theta - 1) = 0 \quad \text{at } r = 1 \quad z > 0 \\ &\theta = Q\delta\left(\frac{1}{\mathrm{B}_1} - \ln r\right) \quad \text{at } z \to -\infty \\ &\theta = 1 + Q\delta\left(\frac{1}{\mathrm{B}_2} - \ln r\right) \quad \text{at } z \to +\infty \\ &\theta = \theta_0 \quad \text{at } r = 1 \quad z = 0 \end{aligned} \tag{5}$$

The non-dimensional variables used above are

$$r = \frac{\bar{r}}{R_2} \quad z = \frac{\bar{z}}{R_2} \quad \delta = \frac{R_1}{R_2} \quad \theta = \frac{T - T_s}{T_w - T_s} \quad \theta_0 = \frac{T_0 - T_s}{T_w - T_s}$$

$$\mathrm{B}_1 = \frac{h_1 R_2}{k} \quad \mathrm{B}_2 = \frac{h_2 R_2}{k} \quad \mathrm{Pe} = \frac{\rho C u R_2}{k}$$

$$Q = \frac{qR_2}{k(T_w - T_s)} \quad .$$

Estimation of quench front temperature is important in predicting the rate at which the coolant quenches the hot surface. The main objective of the present analysis is to obtain the quench front temperature θ_0 in terms of wetside Biot number B_1, dryside Biot number B_2, Peclet number Pe, dimensionless heat flux Q and radius ratio δ.

3 Analytical solution

In order to employ the Wiener–Hopf technique, Eq. (4) is first transformed with a new dependent variable φ, defined by $\theta(r,z) = 1 + (Q\delta/\mathrm{B}_2) - Q\delta\ln r - \varphi(r,z)\mathrm{e}^{-sz}$, in which $s = \mathrm{Pe}/2$. The governing equation (Eq. (4)) then becomes

$$\frac{1}{r}\frac{\partial}{\partial r}\left(r\frac{\partial\varphi}{\partial r}\right) + \frac{\partial^2\varphi}{\partial z^2} - s^2\varphi = 0 \qquad \delta < r < 1 \quad -\infty < z < \infty \tag{6}$$

The boundary conditions in Eq. (5) can be written sequentially as

$$\begin{aligned} &\frac{\partial\varphi}{\partial r} = 0 \quad \text{at } r = \delta \quad -\infty < z < \infty \\ &\frac{\partial\varphi}{\partial r} + \mathrm{B}_1\varphi = \mathrm{B}_1\left[1 + Q\delta\left(\frac{1}{\mathrm{B}_2} - \frac{1}{\mathrm{B}_1}\right)\right]\mathrm{e}^{sz} \quad \text{at } r = 1 \quad z < 0 \\ &\frac{\partial\varphi}{\partial r} + \mathrm{B}_2\varphi = 0 \quad \text{at } r = 1 \quad z > 0 \\ &\varphi = \left[1 + Q\delta\left(\frac{1}{\mathrm{B}_2} - \frac{1}{\mathrm{B}_1}\right)\right]\mathrm{e}^{sz} \quad \text{at } z \to -\infty \\ &\varphi = 0 \quad \text{at } z \to +\infty \\ &\varphi = \varphi_0 = 1 + \frac{Q\delta}{\mathrm{B}_2} - \theta_0 \quad \text{at } r = 1 \quad z = 0 \end{aligned} \tag{7}$$

3.1 Fourier transform

In the next step of the analysis, Fourier transform is used to convert the partial differential equation (Eq. (6)) to an ordinary differential equation. The Fourier transform is defined by

$$\Phi(\alpha, r) = \Phi_+(\alpha, r) + \Phi_-(\alpha, r) = \int_{-\infty}^{\infty} \varphi(r,z)\mathrm{e}^{\mathrm{i}\alpha z}\,\mathrm{d}z \tag{8}$$

with $\Phi_-(\alpha, r) = \int_{-\infty}^{0} \varphi(r,z)\mathrm{e}^{\mathrm{i}\alpha z}\,\mathrm{d}z$,
$\Phi_+(\alpha, r) = \int_{0}^{\infty} \varphi(r,z)\mathrm{e}^{\mathrm{i}\alpha z}\mathrm{d}z$. The parameter α used above is

a complex quantity. The far-field boundary conditions in Eq. (7) indicate that $\varphi(r,z)$ is of the order e^{sz} at $z \to -\infty$, whereas $\varphi(r,z)$ is of the order e^{-sz} at $z \to +\infty$. The above two conditions ensure that the functions $\Phi_+(\alpha, r)$, $\Phi_-(\alpha, r)$ are analytic in the domains D_+ and D_- respectively (Roos 1969, p. 78). The domains D_+ and D_- are defined (Fig. 1(b)) in the entire complex domain as:
D_+: $\mathrm{Im}(\alpha) > -s$, D_- : $\mathrm{Im}(\alpha) < +s$. Applying the Fourier transform, Eq. (6) assumes the form

$$\frac{1}{r}\frac{\partial}{\partial r}\left(r\frac{\partial \Phi}{\partial r}\right) - \gamma^2 \Phi = 0 \tag{9}$$

in which $\gamma = (\alpha^2 + s^2)^{1/2}$. The transformed boundary conditions are

$$\begin{aligned}
&\Phi'(\alpha, \delta) = 0 \\
&\Phi'_-(\alpha, 1) + \mathrm{B}_1 \Phi_-(\alpha, 1) \\
&\quad = -\frac{\mathrm{i}}{\alpha - \mathrm{i}s}\mathrm{B}_1\left[1 + Q\delta\left(\frac{1}{\mathrm{B}_2} - \frac{1}{\mathrm{B}_1}\right)\right] \\
&\Phi'_+(\alpha, 1) + \mathrm{B}_2 \Phi_+(\alpha, 1) = 0
\end{aligned} \tag{10}$$

where prime denotes the transform of r-derivatives of $\varphi(r,z)$. The general solution of the second order ordinary differential equation (Eq. (9)) is

$$\Phi(\alpha, r) = C_1(\alpha) I_0(\gamma r) + C_2(\alpha) K_0(\gamma r) \tag{11}$$

where I_0, K_0 are zero-order modified Bessel functions of first and second kinds respectively. Imposing the boundary conditions of Eq. (10) into Eq. (11) yields

$$\begin{aligned}
&\Phi_+(\alpha, 1) + \left[\frac{1 + \mathrm{B}_1/(\gamma f(\gamma))}{1 + \mathrm{B}_2/(\gamma f(\gamma))}\right]\Phi_-(\alpha, 1) \\
&\quad = -\frac{\mathrm{i}}{\alpha - \mathrm{i}s}\left[\frac{\mathrm{B}_1/(\gamma f(\gamma))}{1 + \mathrm{B}_2/(\gamma f(\gamma))}\right]\left[1 + Q\delta\left(\frac{1}{\mathrm{B}_2} - \frac{1}{\mathrm{B}_1}\right)\right]
\end{aligned} \tag{12}$$

where

$$f(\gamma) = \frac{I_1(\gamma)K_1(\delta\gamma) - I_1(\delta\gamma)K_1(\gamma)}{I_0(\gamma)K_1(\delta\gamma) + I_1(\delta\gamma)K_0(\gamma)}$$

3.2
Wiener–Hopf technique

The key step in successful execution of the Wiener–Hopf technique depends on the factorization of a function, which is analytic in a strip, into the product of two functions that are analytic in the overlapping half-planes. In this context, let

$$K(\alpha) = K_+(\alpha)K_-(\alpha) = \frac{1 + \mathrm{B}_1/(\gamma f(\gamma))}{1 + \mathrm{B}_2/(\gamma f(\gamma))} \tag{13}$$

where the functions $K_+(\alpha), K_-(\alpha)$ are analytic in the domains D_+ and D_- respectively. Now the kernel function $K(\alpha)$, in connection with Eq. (12), is to be decomposed to $K_+(\alpha)$ and $K_-(\alpha)$ in accordance with the Wiener–Hopf technique. This is accomplished by rearranging Eq. (12) to obtain

$$\begin{aligned}
&\frac{\Phi_+(\alpha, 1)}{K_+(\alpha)} - \frac{\mathrm{i}}{\alpha - \mathrm{i}s}\left(\frac{Q\delta}{\mathrm{B}_2} + \frac{\mathrm{B}_1}{\mathrm{B}_1 - \mathrm{B}_2}\right)\left[\frac{1}{K_+(\alpha)} - \frac{1}{K_+(\mathrm{i}s)}\right] \\
&\quad = -\frac{\mathrm{i}}{\alpha - \mathrm{i}s}\left(\frac{Q\delta}{\mathrm{B}_2} + \frac{\mathrm{B}_1}{\mathrm{B}_1 - \mathrm{B}_2}\right)\left[K_-(\alpha) - \frac{1}{K_+(\mathrm{i}s)}\right] \\
&\qquad - \Phi_-(\alpha, 1)K_-(\alpha)
\end{aligned} \tag{14}$$

In Eq. (14), each side characterizes the same 'entire function', through its representation in the upper and lower halves of the α-plane. Since $\Phi_+(\alpha, 1)$ and $\Phi_-(\alpha, 1)$ tend to zero at infinity in their half-planes of analyticity, while $K_+(\alpha)$ and $K_-(\alpha)$ remain bounded, it follows that the entire function vanishes according to Liouville's theorem (Roos 1969, p. 27). Hence, equating both sides of the Eq. (14) to zero, $\Phi_+(\alpha, 1)$ and $\Phi_-(\alpha, 1)$ are determined as

$$\begin{aligned}
\Phi_+(\alpha, 1) &= \frac{\mathrm{i}}{\alpha - \mathrm{i}s}\left(\frac{Q\delta}{\mathrm{B}_2} + \frac{\mathrm{B}_1}{\mathrm{B}_1 - \mathrm{B}_2}\right)\left[1 - \frac{K_+(\alpha)}{K_+(\mathrm{i}s)}\right] \\
\Phi_-(\alpha, 1) &= -\frac{\mathrm{i}}{\alpha - \mathrm{i}s}\left(\frac{Q\delta}{\mathrm{B}_2} + \frac{\mathrm{B}_1}{\mathrm{B}_1 - \mathrm{B}_2}\right)\left[1 - \frac{1}{K_-(\alpha)K_+(\mathrm{i}s)}\right]
\end{aligned} \tag{15}$$

3.3
Quench front temperature

Using the above expressions of $\Phi_+(\alpha, 1)$ and $\Phi_-(\alpha, 1)$, quench front temperature may be obtained by inverting the Fourier transform (Eq. (8)). Such an attempt may become tedious because, in order to perform the Fourier inversion, it would be necessary to evaluate the residues of the function $\Phi(\alpha, 1)$ in the complex domain. In the present paper, alternatively, θ_0 has been calculated in a simple way (Levine 1982) as follows.

$$\begin{aligned}
\Phi_+(\alpha, 1) &= \int_0^\infty \varphi(1, z)\mathrm{e}^{\mathrm{i}\alpha z}\,\mathrm{d}z \\
&= \frac{\mathrm{i}}{\alpha}\varphi(1, 0) - \frac{1}{\mathrm{i}\alpha}\int_0^\infty \frac{\partial \varphi(1, z)}{\partial z}\mathrm{e}^{\mathrm{i}\alpha z}\,\mathrm{d}z
\end{aligned} \tag{16}$$

In the limit $\alpha \to \infty$, the second integral appearing in Eq. (16) vanishes since the quantity $\partial\varphi/\partial z$ is bounded (Levine 1982). Then, from Eqs. (15)–(16) and assuming that $K_+(\alpha)$ approaches unity as $\alpha \to \infty$ (the assumption will be proved later), we obtain

$$\begin{aligned}
\varphi(1, 0) &= \lim_{\alpha \to \infty}\left[-\mathrm{i}\alpha\Phi_+(\alpha, 1)\right] \\
&= \left(\frac{Q\delta}{\mathrm{B}_2} + \frac{\mathrm{B}_1}{\mathrm{B}_1 - \mathrm{B}_2}\right)\left[1 - \frac{1}{K_+(\mathrm{i}s)}\right]
\end{aligned} \tag{17}$$

The quench front temperature then becomes

$$\begin{aligned}
\theta_0 &= 1 + Q\delta/\mathrm{B}_2 - \varphi(1, 0) \\
&= \frac{1}{K_+(\mathrm{i}s)}\left[\frac{Q\delta}{\mathrm{B}_2} + \frac{\mathrm{B}_1}{\mathrm{B}_1 - \mathrm{B}_2}\right] - \frac{\mathrm{B}_2}{\mathrm{B}_1 - \mathrm{B}_2}
\end{aligned} \tag{18}$$

The function $K_+(\mathrm{i}s)$ appearing in Eq. (18) is then derived by decomposing $K(\alpha)$, for which the 'contour integral

approach' has been adopted in the present case. On applying the Cauchy residue theorem within the strip, the function $\ln K(\alpha)$ can be represented by the following contour integral.

$$\ln K(\alpha) = \ln K_+(\alpha) + \ln K_-(\alpha) = \frac{1}{2\pi \mathrm{i}} \int_{C_+} \frac{\ln K(\xi)}{\xi - \alpha} \mathrm{d}\xi - \frac{1}{2\pi \mathrm{i}} \int_{C_-} \frac{\ln K(\xi)}{\xi - \alpha} \mathrm{d}\xi \quad (19)$$

where C_+/C_- is an infinite contour lying inside the strip and passing below/above the point α (Fig. 1b). It may be noted that, due to the asymptotic nature of $\ln K(\alpha)$ function (the order of $\ln K(\alpha)$ being $1/\alpha$), the contribution of vertical sides of the contour to the integral vanishes at $\mathrm{Re}(\alpha) \to \pm\infty$. Equation (19) can be precisely written as

$$\ln K_\pm(\alpha) = \pm \frac{1}{2\pi \mathrm{i}} \int_{C_\pm} \frac{\ln K(\xi)}{\xi - \alpha} \mathrm{d}\xi \quad (20)$$

from which it follows that $K_\pm(\alpha) = 1$ as $\alpha \to \infty$, as assumed earlier. In order to evaluate the function $K_+(\mathrm{i}s)$, the contour C_+ may be shifted to the real axis to yield

$$\ln K_+(\mathrm{i}s) = \frac{1}{2\pi \mathrm{i}} \int_{-\infty}^{+\infty} \frac{\ln K(\xi)}{\xi - \mathrm{i}s} \mathrm{d}\xi \quad (21)$$

Further, due to the even property of the function $\ln K(\xi)$, Eq. (21) thereby reduces to

$$\ln K_+(\mathrm{i}s) = \frac{s}{\pi} \int_0^{\infty} \frac{\ln K(\xi)}{\xi^2 + s^2} \mathrm{d}\xi \quad (22)$$

For computational purposes it is advantageous to transform ξ, by $\xi = s \tan \Omega$, to finally obtain the quench front temperature

$$\theta_0 = \exp\left[-\frac{1}{\pi} \int_0^{\pi/2} \ln\left\{ \frac{1 + \mathrm{B}_1/(sf(\Omega)\sec\Omega)}{1 + \mathrm{B}_2/(sf(\Omega)\sec\Omega)} \right\} \mathrm{d}\Omega \right] \times \left[\frac{Q\delta}{\mathrm{B}_2} + \frac{\mathrm{B}_1}{\mathrm{B}_1 - \mathrm{B}_2} \right] - \frac{\mathrm{B}_2}{\mathrm{B}_1 - \mathrm{B}_2} \quad (23)$$

in which

$$f(\Omega) = \frac{I_1(s\sec\Omega)K_1(s\delta\sec\Omega) - I_1(s\delta\sec\Omega)K_1(s\sec\Omega)}{I_0(s\sec\Omega)K_1(s\delta\sec\Omega) + I_1(s\delta\sec\Omega)K_0(s\sec\Omega)}$$

where I_n, K_n denote the modified Bessel functions of the first and second kinds respectively. It is of interest to examine the limiting solution of the above equation for the case that has been obtained by other investigators, namely, the rewetting of an infinite tube without any heating or precursory cooling. By assigning $Q = 0, \mathrm{B}_2 = 0$ and $Q/\mathrm{B}_2 = 0$ in Eq. (23), the expression for θ_0 reduces to exactly the same as that of Chakrabarti (1986) and Olek (1989) which, in turn, substantiates the present solution. Moreover, the present model simulates the rewetting of a solid rod with an adiabatic dryside (by assigning $Q = 0$, $\mathrm{B}_2 = 0$, $Q/\mathrm{B}_2 = 0$ and $\delta = 0$), that results in

$$\theta_0 = \exp\left[-\frac{1}{\pi} \int_0^{\pi/2} \ln\left\{ 1 + \frac{\mathrm{B}_1}{s\sec\Omega} \frac{I_0(s\sec\Omega)}{I_1(s\sec\Omega)} \right\} \mathrm{d}\Omega \right] \quad (24)$$

which is the same expression as obtained by Evans (1984).

3.4 Critical heat flux

The quench front temperature at the critical (dryout) heat flux has been deduced by specifying $s = 0$ in Eq. (23). Thus, $K_+(\mathrm{i}s)$ simplifies to

$$K_+(\mathrm{i}s) = \exp\left[\frac{1}{\pi} \int_0^{\pi/2} \ln(\mathrm{B}_1/\mathrm{B}_2) \mathrm{d}\Omega \right] = \sqrt{\frac{\mathrm{B}_1}{\mathrm{B}_2}}$$

The quench front temperature at the critical heat flux is finally obtained as

$$\theta_0 = \frac{Q\delta}{\sqrt{\mathrm{B}_1\mathrm{B}_2}} + \frac{\sqrt{\mathrm{B}_2}}{\sqrt{\mathrm{B}_1} + \sqrt{\mathrm{B}_2}} \quad (25)$$

The heat flux Q appearing in Eq. (25) may be regarded as the critical heat flux Q_{cri}, which represents the maximum allowable boundary heat flux so as to prevent the dryout of the coolant.

4 Results and discussion

Reported literature on experimental investigations on quenching (Barnea et al. 1994) reveals the existence of four distinct heat transfer regimes along the wall, the regimes being demarcated by the characteristic hot surface temperature. These four zones are: forced convection of subcooled liquid, nucleate boiling, wet and dry transition boiling and film boiling. Quench front is observed to exist in the transition zone. The heat transfer coefficient in the transition zone is shown to be in the order of 10^5–10^6 W/m^2 K and the vapor cooling heat transfer coefficient in the film boiling zone is in the order of 10^2 W/m^2 K. Hence, in the present analysis the values of B_2 are set equal to $10^{-3}\mathrm{B}_1$. Numerical values of the quench front temperature are obtained from the expressions in Eqs. (23)–(25), for a practical range of model parameters B_1, B_2, Pe and Q. For this purpose, the integrals appearing in Eqs. (23) and (24) have been numerically calculated by Simpson's 1/3 rule with 101 equally spaced base points.

The dependence of quench front temperature on Biot number and dimensionless heat flux is shown in Fig. 2, where θ_0 decreases with increase in Biot number for a given Pe and Q. With fixed material properties and dimensions, Peclet number and Biot number represent the quench front velocity and the heat transfer coefficient respectively. Thus, a higher Biot number results in a higher heat transfer coefficient. This enhanced heat transfer coefficient may cause to decrease θ_0. Further, for a fixed Peclet number, θ_0 increases with increase in Q. Apparently, a higher heat flux causes more heat transfer to the tube and hence this would increase θ_0. The above trends are in

obvious accord with the predictions based on physical ground. Quench front temperature decreases as the Biot number increases, reflecting the fact that a quench front progresses more easily when the heat transfer to the coolant is increased. On a similar ground, conversely, one would conclude that an increasing Q has the opposite effect on the quench front velocity.

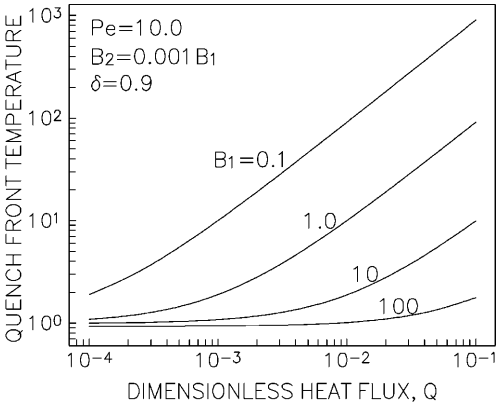

Fig. 2. Quench front temperature for various heat flux and Biot number

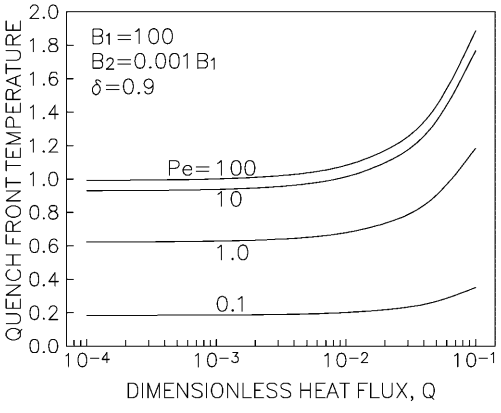

Fig. 3. Quench front temperature for various heat flux and Peclet number

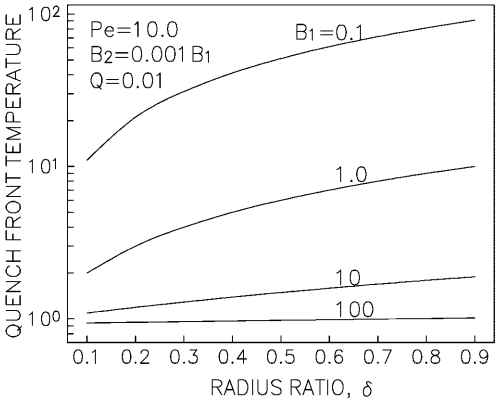

Fig. 4. Quench front temperature variation with radius ratio and Biot number

The variation of quench front temperature with dimensionless heat flux and Peclet number is shown in Fig. 3, for a fixed value of Biot number. Here θ_0 is found to increase with increase in Peclet number (quench front velocity). This may be due to the fact that a higher relative velocity between the tube and the coolant allows less time for sufficient heat transfer to take place, resulting in a higher value of θ_0. The above trend also reflects the fact that, for the same rewetting rate and the physical dimension, an increasing solid thermal diffusivity tends to reduce θ_0. Figure 4 shows the dependence of quench front temperature with the radius ratio δ and Biot number, for fixed values of Pe and Q. In this case θ_0 increases with increase in δ. Evidently, due to the presence of the heat flux on the tube wall, an increase in δ results in an increase in the far-field temperatures which may cause to increase θ_0. Further, an increase in the value of δ means the thickness of the tube decreases and thereby its thermal resistance also decreases. Thus the quench front temperature would increase with increase in δ.

The dependence of quench front temperature on Biot number and dimensionless heat flux is shown in Fig. 5, with Pe = 0. The physical meaning of Pe = 0 is that the quench front ceases to move when Q approaches its critical value. In this case, the surface can no longer be wetted. For

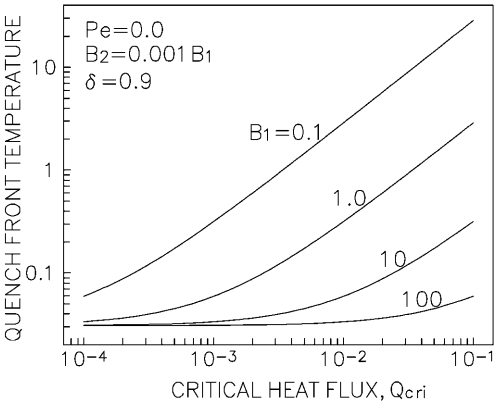

Fig. 5. Quench front temperature at the critical heat flux

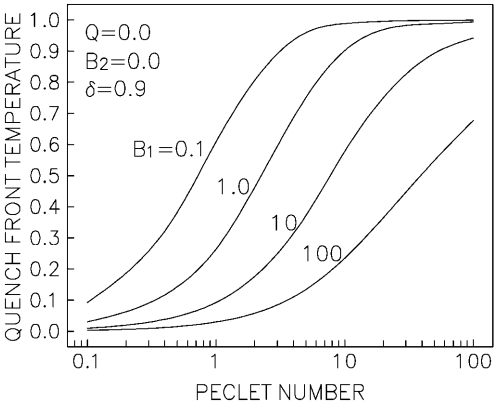

Fig. 6. Quench front temperature variation with Biot and Peclet number for tube

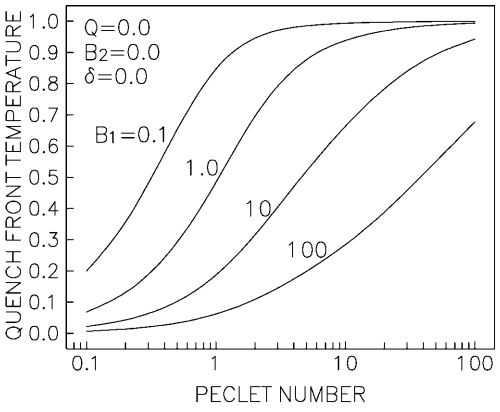

Fig. 7. Quench front temperature variation with Biot and Peclet number for the rod

$Q > Q_{cri}$, the quench front will reverse its direction and the wetted surface will be dried. This is the case that the tube will be heated by a heat flux that exceeds the maximum heat removal capacity by convection and boiling and, thus, dryout would occur. Finally, the model is reduced to the conventional model of a tube without any heating or precursory cooling (by setting $Q = 0$, $B_2 = 0$ and $Q/B_2 = 0$) and illustrated in Fig. 6. Moreover, the present model is reduced to the rewetting of a solid rod with an adiabatic dryside by setting $\delta = 0$ and illustrated in Fig. 7. As expected, in both the cases θ_0 increases with increase in Peclet number and with decrease in Biot number.

The boundary conditions in the present formulation require liquid/vapor temperatures and liquid/vapor heat transfer coefficients as input parameters, these limitations being inherent in a conduction-controlled rewetting model. The arbitrariness of the choice of their values may be eliminated if a conjugate heat transfer model is considered, where the energy equations of solid, liquid and vapor regions need to be solved simultaneously.

References

Barnea Y; Elias E; Shai I (1994) Flow and heat transfer regimes during quenching of hot surfaces. Int J Heat Mass Transfer 37: 1441–1453

Chakrabarti A (1986) The sputtering temperature of a cooling cylindrical rod with an insulated core. Appl Scientific Res 43: 107–113

Chan SH; Zhang W (1994) Rewetting theory and the dryout heat flux of smooth and grooved plates with a uniform heating. ASME J Heat Transfer 116: 173–179

Evans DV (1984) A note on the cooling of a cylinder entering a fluid. IMA J Appl Math 33: 49–54

Levine H (1982) On a mixed boundary value problem of diffusion type. Appl Scientific Res 39: 261–276

Olek S (1988) On the two-region rewetting model with a step change in the heat transfer coefficient. Nuclear Engng Design 108: 315–322

Olek S (1989) Solution to a fuel-and-cladding rewetting model. Int Comm Heat Mass Transfer 16: 143–158

Olek S (1994) Quenching of a composite slab. Int Comm Heat Mass Transfer 21: 333–344

Peng XF; Peterson GP (1992) Analysis of rewetting for surface tension induced flow. ASME J Heat Transfer 114: 703–707

Roos BD (1969) Analytical Functions and Distributions in Physics and Engineering. John Wiley & Sons, New York

Tien CL; Yao LS (1975) Analysis of conduction controlled rewetting of a vertical surface. ASME J Heat Transfer 97: 161–165

Yao LS (1977) Rewetting of a vertical surface with internal heat generation. AIChE Symposium Series 73: 46–50